Journal of Alloys and Compounds 504 (2010) 479–483

Contents lists available at ScienceDirect

Journal of Alloys and Compounds

journal homepage: www.elsevier.com/locate/jallcom

The structural role of manganese ions in some zinc phosphate glasses and glass ceramics

Petru Pascuta[a,*], Gheorghe Borodi[b], Nicolaie Jumate[a], Ioan Vida-Simiti[a], Dan Viorel[a], Eugen Culea[a]

[a] Technical University of Cluj-Napoca, 400020 Cluj-Napoca, Romania
[b] National Institute for R&D of Isotopic and Molecular Technology, P.O. Box 700, RO-400293 Cluj-Napoca, Romania

ARTICLE INFO

Article history:
Received 17 January 2010
Received in revised form 27 May 2010
Accepted 29 May 2010
Available online 11 June 2010

Keywords:
Zinc phosphate glasses
Manganese ions
XRD
SEM
FTIR

ABSTRACT

X-ray diffraction (XRD), scanning electron microscopy (SEM) and Fourier transform infrared (FTIR) spectroscopy measurements have been employed to investigate the samples from the $(MnO)_x\cdot(P_2O_5)_{40}\cdot(ZnO)_{60-x}$ ($0 \le x \le 30$ mol%) system. The samples had a fixed P_2O_5 content of 40 mol% and the MnO:ZnO ratio was varied. The XRD pattern for the prepared samples shows that the vitreous phase is present only for $x \le 20$ mol%. For the sample containing 30 mol% MnO the presence of a crystalline phase was evidenced, namely the manganese phosphate ($Mn_2P_2O_7$) embedded in an amorphous matrix. In this case the XRD patterns show the presence of nanometer crystals (56 nm) in a glassy matrix. The estimated amount of the crystalline phase was 74%. The electron micrographs show the structural evolution of the studied samples from a completely amorphous state (for the samples up to 20 mol% MnO) to a partly crystalline one (for the sample with 30 mol% MnO). FTIR data revealed that the short-range order of the glassy matrix is affected by the addition of the MnO to the $(P_2O_5)_{40}\cdot(ZnO)_{60}$ host glass matrix. The compositional dependence of the different structural units which appear in the studied samples was followed. FTIR spectroscopy data suggest that the manganese ions play the network modifier role in the studied samples.

1. Introduction

Glasses based on P_2O_5 are both scientifically and technologically important materials because they generally offer some physical properties better than other glasses. Thus, phosphate glasses show high thermal expansion coefficients, low melting and softening temperatures, high electrical conductivity, ultraviolet transmission and optical characteristic, etc. [1–7]. Because of these particular properties phosphate glasses are ideal materials for many applications such as laser hosts, glass-to-metal seals solid electrolytes and low frequency waveguides, photoconductors, nuclear waste immobilization matrices and as biomaterials [4,8–11].

The structural role of ZnO in many oxide glasses is unique since zinc oxide can act both as a glass former and a glass modifier. As glass former, ZnO enters the network with ZnO_4 structural units. As network modifier, zinc ion is octahedrally coordinated and behaves like the conventional alkali oxide modifiers [12].

The introduction of transition metal ions (TMI), such as manganese, iron, copper, vanadium, etc., in glasses leads to changes in the glass structure and confers interesting electrical, optical and magnetic properties [13–22]. TMI exist in different valence states with different coordinations in glasses. Thus, the manganese ions appear as Mn^{3+} with octahedral coordination in borate glasses and as Mn^{2+} with both tetrahedral and octahedral environments in silicate and germanate glasses. The content of TMI in different coordinations and valence states existing in the glass depends upon the quantitative properties of modifiers and glass formers, the size of the ions in the glass structure, their field strength, the mobility of the modifier cation, etc. Having in view that the addition of TMI to glasses usually induces significant changes in their electrical, optical and magnetic behaviour, opening thus opportunities in the finding of new applications, careful structural investigations of glasses containing TMI become necessary. In order to obtain further information on the structural role of manganese ions in zinc phosphate glasses and glass ceramics, the new $(MnO)_x\cdot(P_2O_5)_{40}\cdot(ZnO)_{60-x}$ system was prepared and investigated by means of XRD, SEM and FTIR spectroscopy measurements.

2. Experimental

Glasses of the $(MnO)_x\cdot(P_2O_5)_{40}\cdot(ZnO)_{60-x}$ ($0 \le x \le 30$ mol%) system were prepared using MnO, P_2O_5 and ZnO of high purity (99.9%) in suitable proportion. The mechanically homogenized mixtures were melted in sintered corundum crucibles at 1100 °C, in an electric furnace. The samples were put into the electric furnace directly at this temperature. After 10 min, the molten material was quenched at room temperature by pouring onto a stainless-steel plate.

* Corresponding author. Tel.: +40 264 401 262; fax: +40 264 595 355.
E-mail address: petru.pascuta@phys.utcluj.ro (P. Pascuta).

0925-8388/$ – see front matter © 2010 Elsevier B.V. All rights reserved.
doi:10.1016/j.jallcom.2010.05.147

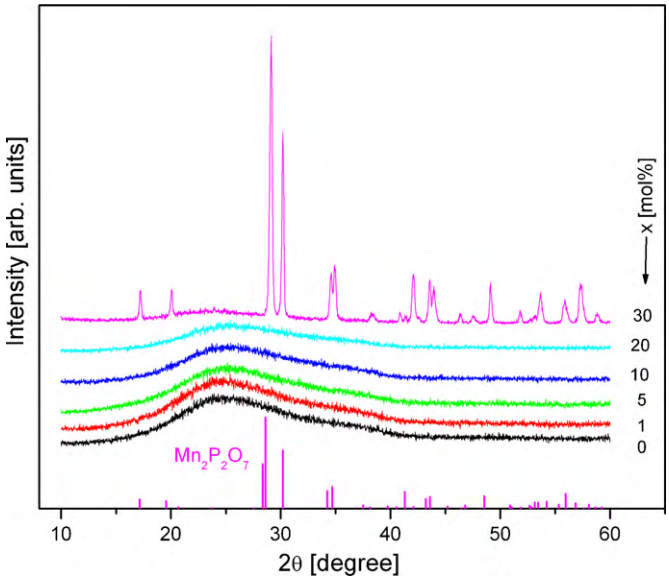

Fig. 1. The XRD patterns of $(MnO)_x{\cdot}(P_2O_5)_{40}{\cdot}(ZnO)_{(60-x)}$ samples.

The X-Ray diffraction measurements of the samples were performed with a XRD – 6000 Shimadzu diffractometer with a monochromator of graphite for Cu-Kα radiation (λ = 1.54060 Å) at room temperature.

Microscopic examination of the samples was made with a Jeol JSM 5600-LV scanning electron microscope.

The FTIR absorption spectra of the studied glasses and glass ceramics were obtained in the 360–1500 cm^{-1} spectral range with a resolution of 2 cm^{-1} using a JASCO FTIR 6200 spectrometer. The IR absorption measurements were done using the KBr pellet technique. In order to obtain good quality spectra, the samples were crushed in an agate mortar to obtain particles of micrometer size. This procedure was applied every time to fragments of bulk glass to avoid structural modifications due to ambient moisture. At last two spectra for each sample were recorded. The spectra were normalized by making the absorption of any spectrum to vary from zero to one arbiter units. Such normalization effect was necessary to eliminate the concentration effect of the powder sample in the KBr disc.

3. Results and discussion

3.1. XRD data

The XRD patterns of $(MnO)_x{\cdot}(P_2O_5)_{40}{\cdot}(ZnO)_{60-x}$ glasses with various contents of manganese oxide ($0 \le x \le 30$ mol%) are presented in Fig. 1. These patterns show that crystalline phase is present only in the sample with $x = 30$ mol%. Up to this concentration glasses were obtained. For the sample with the 30 mol% MnO content the vitreous phase coexists with a crystalline phase and the pattern shows large maxima overlapped with the peaks characteristic to the crystalline phase. All detectable peaks can be indexed as belonging to the $Mn_2P_2O_7$ crystal in the standard data (PDF#771243). The results indicated that the $Mn_2P_2O_7$ crystal structure is monoclinic with the C2/m space group. It is well known that $Mn_2P_2O_7$ has a wide range of applications and can be used as catalyst, reactant in ionic conditions, intercalation reactions, laser host, ceramic dye pigment, ion exchanger, ionic conductor and as super phosphate fertilizer [23,24]. The lattice parameters for this phase were determined and present the following values: $a = 6.635$ Å, $b = 8.584$ Å, $c = 4.641$ and $\beta = 102.70^\circ$ very close to those of the standard data PDF#771243 ($a = 6.633$ Å, $b = 8.584$ Å, $c = 4.646$ and $\beta = 102.67^\circ$). For the sample with 30 mol% MnO, from the full width at half maximum for all peaks of the refined diffraction line profiles, the average crystallite size of the crystalline phase has been determined by using the Debye–Scherrer formula given by [25]:

$$D = \frac{\lambda \cdot K}{\beta \cdot \cos\theta}$$

where D is the apparent volume-weighted crystallite size, λ is the X-rays wavelength (1.54060 Å, in this case), $K = 0.89$ (the Scherrer constant), β is the width of line at the half maximum intensity in radians and θ is the Bragg angle. From Debye–Scherrer calculation, the average crystallite size of sample with 30 mol% MnO is 56 nm, so it lies in the nano-range. The degree of crystallinity was estimated using the relationship

$$X_c = \frac{I_c}{I_c + I_a} \times 100$$

where X_c is the crystallinity, I_c is the integrated intensity of the crystalline phase, $I_c = I_{a0} - I_a$, I_{a0} and I_a are the integrated intensities of the amorphous phase for a completely amorphous specimen and for the specimen with a crystallinity that were to be determined. In our case, the crystallinity for the sample with 30 mol% MnO was determined considering the sample with 20 mol% MnO as the completely amorphous specimen. Thus, for the sample with 30 mol% MnO we obtained 74% crystalline phase and 26% amorphous phase.

3.2. SEM data

To further understand the structure of the studied glass and glass ceramic samples, microstructural analysis was performed by SEM. Fig. 2a and b shows SEM of the samples with $x = 20$ mol% and $x = 30$ mol%. The micrograph of the sample with 20 mol% MnO (Fig. 2a) does not exhibit the presence of any microstructure being characteristic of an amorphous phase. The SEM recorded for the glass ceramics sample (Fig. 2b) shows crystalline agglomerates of

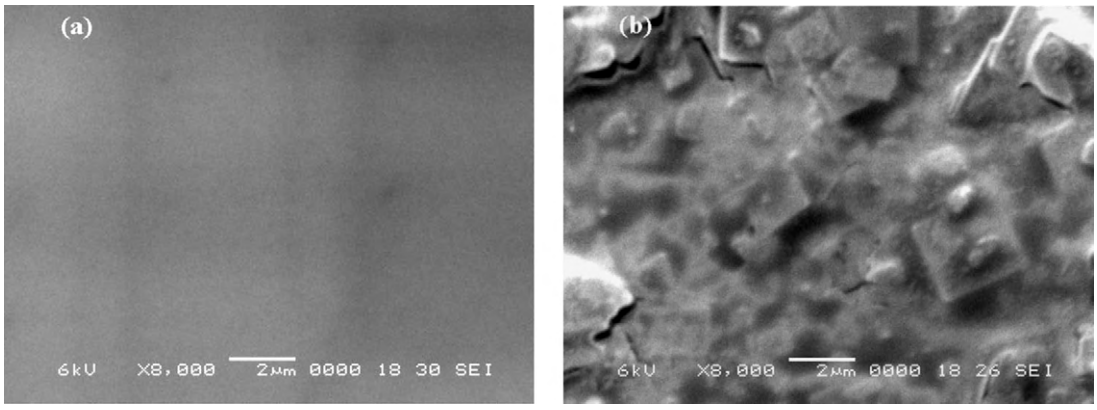

Fig. 2. SEM for sample containing 20 mol% MnO (a) and sample containing 30 mol% MnO (b).

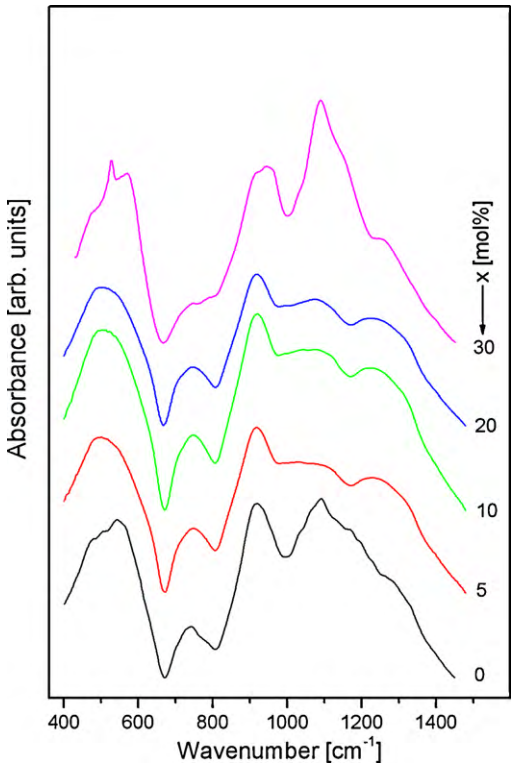

Fig. 3. FTIR spectra of the $(MnO)_x{\cdot}(P_2O_5)_{40}{\cdot}(ZnO)_{(60-x)}$ samples.

varied sizes, of different shapes, surrounded by the amorphous phase. These results are in agreement with the information provided by the XRD patterns.

3.3. FTIR data

In order to determine the main features concerning the local structure of the glasses, FTIR absorption measurements were carried out. The spectroscopic data available from these measurements provide important information concerning the local structure. This is additionally valuable in the case of amorphous systems for which the most powerful method of structure determination – X-ray diffraction – is ineffective. The experimental FTIR spectra of $(MnO)_x{\cdot}(P_2O_5)_{40}{\cdot}(ZnO)_{60-x}$ system with various content of manganese oxide ($0 \le x \le 30$ mol%) are presented in Fig. 3. Since the majority of the IR bands are very broad and asymmetric presenting also some shoulders, a deconvolution of the experimental spectra was necessary. The deconvolution procedure was made with the Spectra Manager program using a Gaussian type function that allowed us a better identification of all the bands which appear in these spectra and their assignments. The deconvolution process makes it possible to calculate the relative area of each component band. Each component band is related to some type of vibration in specific structural groups. The concentration of the structural group is proportional to the relative areas of its component bands. The deconvolution parameters, the band centers *C* and the relative area *A* as well as the bands assignments for the studied samples are given in Table 1. Fig. 3 shows the deconvolution in Gaussian bands of the spectrum for binary the $(P_2O_5)_{40}{\cdot}(ZnO)_{60}$ glass matrix (Fig. 4a) and for the $(MnO)_{30}{\cdot}(P_2O_5)_{40}{\cdot}(ZnO)_{30}$ glass ceramic (Fig. 4b). The absorption band at ~479 cm^{-1} is assigned to harmonics of bending vibrations of O=P–O linkages [26] while the band from ~574 cm^{-1} may be due to the bridging phosphorous, O–P–O [27]. The amount of bridging phosphorous, as indicated by the relative area, shows a maximum value for the glass containing 10 mol% MnO (Fig. 5a). The considerable change in the amount of these bridges may reflect the modification in the glass structure due to the depolymerization of the phosphate matrix with increasing MnO content. The bands from ~722 cm^{-1} and ~762 cm^{-1} are assigned to the P–O–P sym-

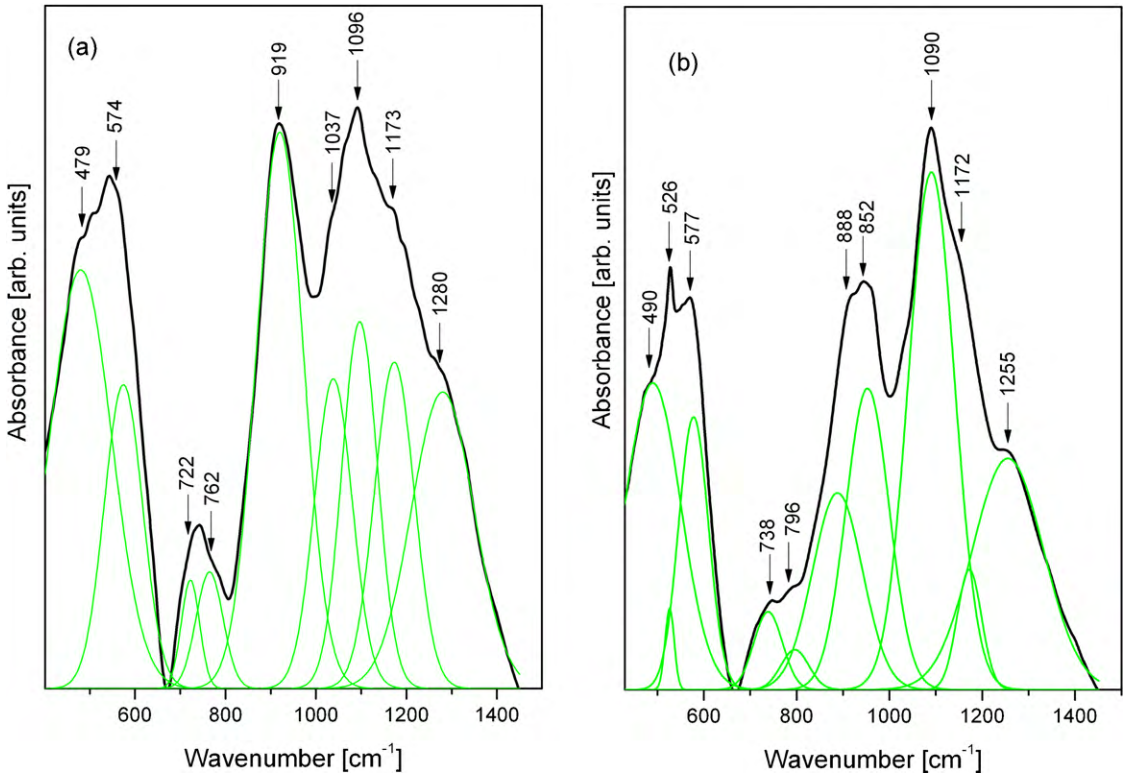

Fig. 4. Deconvoluted FTIR spectra of the $(MnO)_x{\cdot}(P_2O_5)_{40}{\cdot}(ZnO)_{(60-x)}$ samples using a Gaussian type function for $x = 0$ mol% (a) and for $x = 30$ mol% (b).

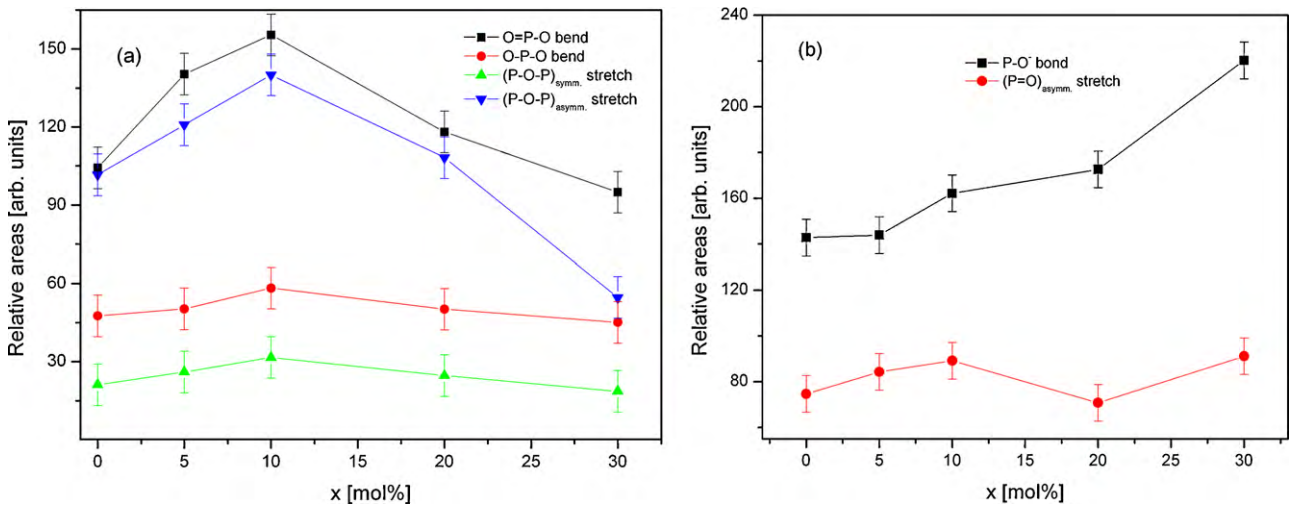

Fig. 5. Dependence of the relative area corresponding to different P–O vibrational modes on MnO content. The lines are drawn as a guide for the eyes.

Table 1
Deconvolution parameters (the band centers *C* and the relative area *A*) and the bands assignments for the $(MnO)_x\cdot(P_2O_5)_{40}\cdot(ZnO)_{(60-x)}$ samples.

$x=0$		$x=5$		$x=10$		$x=20$		$x=30$		Assignment
C	*A*	*C*	*A*	*C*	*A*	*C*	*A*	*C*	*A*	
479	104.3	486	140.3	493	155.4	491	118.1	490	94.9	O=P–O bend
–	–	–	–	–	–	–	–	526	4.1	Mn–O bond
574	47.6	588	50.2	590	58.2	588	50.1	577	45.1	O–P–O bend
722	7.4	711	5.5	712	7.1	709	5.3	738	12.4	$(P–O–P)_{symm.}$ stretch
762	13.7	755	20.5	754	24.5	754	19.3	796	6.2	
919	101.6	919	120.9	920	140	919	108.2	888	54.6	$(P–O–P)_{asymm.}$ stretch
1037	44.7	1019	29.4	1019	20.5	1016	41.9	952	72.3	$(PO_3)^{2-}$ stretch (Q^1)
1096	49.5	1084	57.9	1082	60.2	1077	59.8	1090	131.5	$(PO_4)^{3-}{}_{asymm.}$ stretch (Q^0)
1173	48.6	1182	56.6	1182	81.4	1177	70.9	1172	16.4	$(PO_2)^-$ stretch (Q^2)
1280	74.7	1292	84.3	1299	89.2	1295	70.8	1255	91.2	$(P=O)_{asymm.}$ stretch

metric stretching vibrations [28] while the band from ~919 cm^{-1} is due to the asymmetric stretching vibration of P–O–P [29]. The relative area of these bands increases with the MnO content up to 10 mol% and decreases for higher contents of manganese ions (Fig. 5b). The decreases in the relative area may be due to the formation of the P–O–Mn bonds at the expense of the rest of the P–O–P linkages. The formation of bridging oxygen (Mn–O–P) would increase the cross-link density of the glass network improving the chemical durability of the glasses. The bands from ~1037 cm^{-1}, ~1096 cm^{-1} and ~1173 cm^{-1} are due to the stretching vibrations of $(PO_3)^{2-}$ in Q^1, the asymmetric stretching vibration of $(PO_4)^{3-}$ in Q^0 and the stretching vibrations of $(PO_2)^-$ in Q^2 [4]. The presence of these bands suggests the ionic character of the samples. Fig. 5b shows the dependence of the relative area corresponding to the $P–O^-$ ionic bond of the MnO content. The relative areas of these bands increase with increasing of the manganese ions content in the whole concentration range. This means that the ionic character of the $MnO–P_2O_5–ZnO$ glasses increases with the MnO content increase confirming the role of manganese ions as glass modifier. This fact indicates an increase in the number of non-bridging oxygen ions due to depolymerization of the glass network [26]. The band from ~1280 cm^{-1} is due to the asymmetric stretching vibration of the P=O bond [4]. Fig. 4b displays the dependence of the relative area of the band corresponding to the P=O bond on MnO content. It is interesting to observe that the relative area of this band increase up to 10 mol% MnO, for $10 < x < 20$ mol% decrease, and for $x > 20$ mol% increase. The decrease of this relative area indicates that the addition of MnO to the $(P_2O_5)_{40}\cdot(ZnO)_{60}$ glass network probably leads to more breakdowns of the P=O bonds and formation of the P–O–Mn bonds.

4. Conclusions

Homogeneous glasses of the $(MnO)_x\cdot(P_2O_5)_{40}\cdot(ZnO)_{60-x}$ system were obtained within the $0 \le x \le 20$ mol% composition range while the sample with 30 mol% MnO was a glass ceramic. The crystalline phase of the glass ceramic sample was identified to be the $Mn_2P_2O_7$ which crystallizes in the monoclinic system. About 74% of the glass ceramic sample crystallizes as manganese phosphate and the rest remains in the amorphous state. The crystallite size of the manganese phosphate is 56 nm, so it lies in the nano-range. The SEM investigation shows the evolution of the structural modifications with respect to the MnO content of the studied samples: from a completely amorphous to a partly crystalline state. The FTIR data show that the controlled addition of MnO in the studied glasses generates several rearrangements in the network structure at the short-range order level. So, the manganese oxide plays the role of vitreous network modifier in the studied glasses. Thus, at higher contents of manganese ions the P=O bonds are breaking; the P–O–P bonds are replaced by P–O–Mn bonds, which improve the chemical stability of these glasses. The ionic character of the studied glasses increases as the MnO content increases. This fact indicates an increase in the number of non-bridging oxygen ions due to depolymerization of the glass network.

Acknowledgement

This work was supported by CNCSIS – UEFISCSU, project number PNII – IDEI 226/2008, contract number 532/2009.

References

[1] M. Seshadri, K.V. Rao, J.L. Rao, Y.C. Ratnakaram, J. Alloys Compd. 476 (2009) 263–270.
[2] A. Kermaoui, F. Pellé, J. Alloys Compd. 469 (2009) 601–608.
[3] S. Rani, S. Sanghi, A. Agarwal, N. Ahlawat, J. Alloys Compd. 477 (2009) 504–509.
[4] S. Marzouk, Mater. Chem. Phys. 114 (2009) 188–193.
[5] Z. Mazurak, S. Bodył, R. Lisiecki, J. Gabryś-Pisarska, M. Czaja, Opt. Mater. 32 (2010) 547–553.
[6] R. Praveena, K.H. Jang, C.K. Jayasankar, H.J. Seo, J. Alloys Compd. 496 (2010) 335–340.
[7] B. Eraiah, R.V. Anavekar, J. Alloys Compd. 489 (2010) 325–327.
[8] X. Liang, S. Yuan, Y. Yang, G. Chen, J. Lumin. 130 (2010) 429–433.
[9] E. Leonardi, G. Ciapetti, N. Baldini, G. Novajra, E. Verné, F. Baino, C. Vitale-Brovarone, Acta Biomater. 6 (2010) 598–606.
[10] M. Sitarz, K. Bulat, M. Szumera, J. Non-Cryst. Solids 356 (2010) 224–231.
[11] D.V.R. Murthy, A.M. Babu, B.C. Jamalaiah, L.R. Moorthy, M. Jayasimhadri, K. Jang, H.S. Lee, S.S. Yi, J.H. Jeong, J. Alloys Compd. 491 (2010) 349–353.
[12] M.S. Reddy, G.M. Krishna, N. Veeraiah, J. Phys. Chem. Solids 67 (2006) 789–795.
[13] I.G. Austin, N.F. Mott, Adv. Phys. 18 (1969) 41–102.
[14] M. Sayer, A. Mansingh, Phys. Rev. B 6 (1972) 4629–4643.
[15] A. Ghosh, J. Appl. Phys. 66 (1989) 2425–2429.
[16] A. Ghosh, J. Phys.: Condens. Matter 1 (1989) 7819–7828.
[17] A. Ghosh, Phys. Rev. B 48 (1993) 9388–9393.
[18] S. Sen, A. Ghosh, J. Phys: Condens. Matter 11 (1999) 1529–1536.
[19] I. Ardelean, C. Andronache, P. Pascuta, Mod. Phys. Lett. B 17 (2003) 1271–1275.
[20] I. Ardelean, N. Muresan, P. Pascuta, Mater. Chem. Phys. 101 (2007) 177–181.
[21] N.K. Mohan, M.R. Reddy, C.K. Jayasankar, N. Veeraiah, J. Alloys Compd. 458 (2008) 66–76.
[22] S. Aloka Ghosh, A. Bhattacharya, Ghosh, J. Alloys Compd. 490 (2010) 480–483.
[23] H. Onoda, K. Kojima, H. Nariai, J. Alloys Compd. 408–412 (2006) 568–572.
[24] B. Boonchom, S. Youngme, S. Maensiri, C. Danvirutai, J. Alloys Compd. 454 (2008) 78–82.
[25] X.R.D.P. Scherrer, Nachr. Ges. Göttingen, Wiss. Math.-Physik. Klasse 2 (1918) 98–100.
[26] H. Doweidar, Y.M. Moustafa, K. El-Egili, I. Abbas, Vib. Spectrosc. 37 (2005) 91–96.
[27] A.M. Efimov, J. Non-Cryst. Solids 209 (1997) 209–226.
[28] P. Subbalakshmi, N. Veeraiah, J. Non-Cryst. Solids 298 (2002) 89–98.
[29] B.H. Jung, D.N. Kim, H.S. Kim, J. Non-Cryst. Solids 351 (2005) 3356–3360.